

Supplementary Information for:

Biomechanical constraints reverse scaling of the activity time in carnivores

Matteo Rizzuto^{1,*}, Chris Carbone², Samraat Pawar^{1,†}¹*Department of Life Sciences, Imperial College London, Silwood Park Campus, Ascot, UK*²*Institute of Zoology, Zoological Society of London, Regent's Park, London, UK*

***Corresponding author.** *Current Address: Department of Biology, Memorial University of Newfoundland, 230 Elizabeth Ave, St. John's, NL A1B 3X9, Canada; E-mail: mrizzuto@mun.ca*

†Corresponding author. *E-mail: s.pawar@imperial.ac.uk*

1 The activity budget model

Here we detail the derivation and parameterizations of our activity budget model.

1.1 Model derivation

We are interested in the net energy (Joules, J) budget of an individual over some time scale (e.g., one day). The energy budget for an individual is:

$$E_N = E_G - E_L \quad (1)$$

where E_N , E_G and E_L are the individual's net energy flux, energy gain and energy loss, respectively, in the given time period. Then, given that the two sources of daily energy loss are for maintaining metabolism at rest (E_B) and the loss when actively moving around (E_A), a large proportion of which is usually invested in searching for resources (Holling, 1966; Pawar *et al.*, 2015),

$$E_N = E_G - E_B - E_A \quad (2)$$

And the total time-budget of an individual is,

$$T_{tot} = T_B + T_A \quad (3)$$

where T_{tot} , T_B and T_A are total, resting and active time duration, respectively. Let us also define energy intake per unit time (intake rate) as I , energy loss rate while resting as B and energy loss rate while actively moving as A . Then, $E_G = I \cdot T_A$, $E_B = B \cdot T_B$, $E_A = A \cdot T_A$, and Eqn (2) can be expressed as,

$$E_N = T_A I - T_B B - T_A A$$

Or, because $T_B = T_{tot} - T_A$ (Eqn (3)),

$$E_N = T_A I - (T_{tot} - T_A) B - T_A A \quad (4)$$

Note that the relationship $E_G = I \cdot T_A$ is valid only if I is measured as field consumption rate, where energy intake is averaged over the total activity time, which is the sum of the time spent searching (T_S) and handling/ingesting (T_I), i.e., $T_A = T_S + T_I$ (Holling, 1966; Pawar *et al.*, 2015)).

Finally, solving for the amount of time that the individual needs to be active (T_A) for maintaining energy balance ($E_N = 0$), we get,

$$T_A = \frac{T_{tot} B}{I + B - A}$$

This can be expressed as the proportion of time active ($T_p = T_A/T_{tot}$):

$$T_p = \frac{B}{I + B - A} \quad (5)$$

This equation sets a *lower bound* on the proportion of time spent active by the average individual, as it satisfies the condition for maintenance of individual biomass. Thus, while confronting the model with empirical data, we expect the right hand side of Eqn (5) to be appropriate for predicting the lower ranges or bounds of activity times in each species. A similar model was used by Gorman *et al.* (1998).

1.1.1 Size-scaling of the energy budget

We now incorporate the effect of body-size on B , A and I in Eqn (5) using metabolic scaling theory. The parameter values for the following scaling models are given in section 1.2.1 and Table S1.

For energy loss rate while resting (B), we use the well-established model for mammalian resting metabolic rate:

$$B = B_0 m^z \quad (6)$$

where m is the body mass of the consumer (Peters, 1983; Kolokotronis *et al.*, 2010).

For energy loss rate while moving (A), we use Taylor *et al.*'s (1982) model:

$$A = A_{0,1} m^{a_1} v + A_{0,2} m^{a_2} \quad (7)$$

where $A_{0,1} \neq A_{0,2}$ and $a_1 \neq a_2$. The first term of the sum on the right hand side of this equation represents the incremental cost of movement — the cost of moving at velocity, v (in $\text{m} \cdot \text{s}^{-1}$). The cost scales with body mass m with intercept and slope $A_{0,1}$ and a_1 respectively. The second term in the equation is an “extrapolated zero speed cost” — the cost of initiating movement which scales with m with intercept and slope $A_{0,2}$ and a_2 respectively (Taylor *et al.*, 1982). Velocity in walking/running animal itself scales with body mass as (Garland, 1983)

$$v = v_0 m^{p_v}, \quad (8)$$

Substituting Eqn (8) into (7) gives

$$A = A_{0,1} v_0 m^{a_1 + p_v} + A_{0,2} m^{a_2} \quad (9)$$

Because our focus is on terrestrial predators, **for energy intake rate (I)**, we start with the general field consumption rate model of Pawar *et al.*, 2012 for 2D (in two-dimensional in euclidean space) consumers-resource interactions,

$$c = 2v_r df(.)x_R \quad (10)$$

where, c is consumption rate ($\text{kg} \cdot \text{s}^{-1}$) v_r is relative velocity between the consumer and resource, d is the reaction distance (minimum distance to detect and react to prey), $f(.)$ is the prey risk function that determines functional response of the consumer (due to the constraints of the consumer's handling time), and x_R is the resource biomass density. We now show how the equation for intake rate in energy units (I) can be obtained from Eqn (10).

Assuming random movement of consumer and resource individuals in the landscape, relative velocity v_r is the square root of the sum of the average velocities of consumer and the resource individuals ($v_r = \sqrt{v^2 + v_R^2}$) (Pawar *et al.*, 2012; Dell *et al.*, 2014). Terrestrial carnivores tend to move around widely in their search for prey which are usually smaller than themselves and restricted to patches. Therefore, we assume that prey can be considered relatively “sessile” with

respect to their consumer such that $v \gg v_R$ in the search/foraging phase of the predator-prey interaction (ignoring velocity differences in the post-encounter phase). That is, $v_r \approx v$ (effectively, “grazing”; Pawar *et al.*, 2012, 2015; Dell *et al.*, 2014), and thus can consider just the scaling of consumer velocity v (Eqn (8)).

For *scaling of reaction distance*, we use (Pawar *et al.*, 2012):

$$d = d_0 m^{2p_d} k^{p_d} \quad (11)$$

where d_0 and p_d are a scaling constant and exponent respectively, and $k = \frac{m_R}{m}$, is the prey-predator body size-ratio. Mass of prey m_R typically scales with predator mass m (Peters, 1983; Pawar *et al.*, 2012) as,

$$m_R = k_0 m^{p_k} \quad (12)$$

So we can rewrite size-ratio $k = \frac{m_R}{m}$ as a scaling function of the consumer’s mass,

$$k = \frac{m_R}{m} = k_0 m^{p_k - 1}$$

Substituting this into Eqn (11) and simplifying then gives,

$$d = d_0 k_0^{p_d} m^{p_d(1+p_k)} \quad (13)$$

For the *scaling of prey biomass abundance*, we use (Peters, 1983; Brown *et al.*, 2004; Carbone *et al.*, 2007b):

$$x_R = x_0 m_R^{1-p_x} \quad (14)$$

Again, substituting the prey-predator scaling relationship, Eqn (12), into (14) gives

$$x_R = x_0 k_0^{1-p_x} m^{p_k(1-p_x)} \quad (15)$$

Substituting Eqns (8), (13) and (15) into (10), setting $f(.) = 1$ and simplifying, we get

$$c = 2v_0 d_0 x_0 k_0^{1-p_x+p_d} m^{p_v+p_d(1+p_k)+p_k(1-p_x)} \quad (16)$$

The rationale behind setting $f(.) = 1$ is that resources/prey are relatively rare under field conditions and therefore handling time is not a dominant constraint (e.e., the Type I functional response is relevant). Converting biomass into energy units (Section 1.2.1) then gives the scaling of intake rate:

$$I = v_0 I_0 m^{p_v+p_d(1+p_k)+p_k(1-p_x)} \quad (17)$$

where

$$I_0 = 2d_0 x_0 k_0^{1-p_x+p_d} \quad (18)$$

Thus, both the scaling constant and exponent of intake rate depend upon the scaling of size-ratio and detection distance.

1.2 Model analysis

Substituting eqns (6), (9) and (17) into (5) gives the effect of body size and size-ratios on proportion of time active:

$$T_p = \frac{B_0 m^z}{v_0 I_0 m^{p_v+p_d(1+p_k)+p_k(1-p_x)} + B_0 m^z - (A_{0,1} v_0 m^{a_1+p_v} + A_{0,2} m^{a_2})} \quad (19)$$

We can combine the abundance, size-ratio, and reaction distance scaling constants in Eqn 19 to get,

$$T_p = \frac{B_0 m^z}{v_0 I_0 m^{p_v+p_I} + B_0 m^z - (A_{0,1} v_0 m^{a_1+p_v} + A_{0,2} m^{a_2})} \quad (20)$$

where

$$p_I = p_d(1 + p_k) + p_k(1 - p_x)$$

$$\frac{-A_{01}m^{a+p_v}v_0(a + p_v) - A_{02}am^a + B_0m^z z + I_0m^{p_I+p_v}v_0(p_I + p_v) + z(A_{01}m^{a+p_v}v_0 + A_{02}m^a - B_0m^z - I_0m^{p_I+p_v}v_0)}{m(A_{01}m^{a+p_v}v_0 + A_{02}m^a - B_0m^z - I_0m^{p_I+p_v}v_0)}$$

To derive predictions for the relationship between body size and proportion of activity time (T_p) and the underlying intake rate (I), we numerically evaluated Eqns (19) and (17). We focused on the contribution of scaling of the exponents of reaction distance, size ratio, and resource abundance to both these measures (main text Fig. 1). The scaling of the other components, including velocity, are relatively well known, especially for mammals. In addition, we note that the predictions for the scaling of T_p and I are relatively insensitive to the velocity because it contributes to both, energy use (Eqns (7) and (9)) and intake Eqn (17).

While we focus mainly on the value of the scaling exponent p_d , it is important to note that intercept value for detection distance (d_0) also plays a role in determining how far and well animals can see. This is, however, negligible compared to that of the scaling exponent, due to the two relationships crossing near a body weight value of 1 kg (see main text Fig. 1, panel b). Varying the value of d_0 varies where the switch in scaling occurs in the 1–10 kg range, but does not otherwise affect the behaviour of the two relationships.

1.2.1 Parameterizations

We now detail parameterizations of the above size-scaling models (see Table S1).

For **Rate of energy use while resting** B , we re-analyzed the data from Kolokotronis *et al.* 2010, dropping aquatic carnivores and bears (omnivores – see above), which gives (B in $\text{J} \cdot \text{s}^{-1}$),

$$B = 3.0 \cdot m^{0.73}$$

These parameter values are very similar to the those reported by Peters (1983).

For **Rate of energy use while active** A , we use Taylor *et al.*'s (1982) original equation, re-expressed in $\text{J} \cdot \text{s}^{-1}$ from original $\text{J} \cdot (\text{kg} \cdot \text{s})^{-1}$,

$$A = 10.7 \cdot m^{0.684} \cdot v + 6.03 \cdot m^{0.697}$$

For velocity we use (Taylor *et al.*, 1982),

$$v = 0.25 \cdot m^{0.24}$$

For **Energy Intake rate** I , we parameterize the components of Eqn 17 & 18 as follows. For velocity we use (Taylor *et al.*, 1982) as above: $v = 0.25 \cdot m^{0.24}$. For reaction distance we use (Pawar *et al.*, 2012):

$$d = 1.62 \cdot m^{0.21}$$

For size-ratio (k) scaling (Eqn 12), we use (Peters, 1983):

$$m_R = 0.109 \cdot m^{1.16}$$

For prey biomass abundance, we use (Carbone *et al.*, 2007b; Pawar *et al.*, 2012),

$$x_R = 0.002 \cdot m_R^{1-0.79}$$

Finally, we convert the resulting c ($\text{kg} \cdot \text{s}^{-1}$) based on these parameterizations to I ($\text{J} \cdot \text{s}^{-1}$) assuming $1 \text{ kg} = 7 \cdot 10^6 \text{ J}$ (Peters, 1983).

Table S1: Parameterizations for the scaling relationships underlying the activity budget.

Trait	Parameters	Value \pm 95% CI	Units (SI)	Mass range (kg)	Source
Resting Metabolic rate	B_0	3.00 (xx, xx)	$\text{J} \cdot \text{s}^{-1}$	xx-xx	Kolokotronis <i>et al.</i> , 2010
	z	0.73 ± 0.08		xx-xx	
Incremental cost of movement	$A_{0,1}$	10.7 (10.1, 11.4)	$\text{J} \cdot \text{s}^{-1}$	0.0072 - 254	Taylor <i>et al.</i> , 1982
	a_1	0.684 ± 0.023		0.0072 - 254	
Cost of initiating movement	$A_{0,2}$	6.03 (5.6, 6.7)	$\text{J} \cdot \text{s}^{-1}$	0.0072 - 254	Taylor <i>et al.</i> , 1982
	a_2	0.697 ± 0.042		0.0072 - 254	
Body velocity	v_0	0.25	$\text{m} \cdot \text{s}^{-1}$	0.056 - 6000	Peters, 1983; Carbone <i>et al.</i> , 2007b
	p_v	0.24 ± 0.08		0.056 - 6000	
Detection distance	d_0	1.62	m	3.10E^{-8} - 109	Pawar <i>et al.</i> , 2012
	p_d	0.21 ± 0.08		3.10E^{-8} - 109	
Prey abundance	x_0	0.002	individuals $\cdot \text{m}^{-2}$	1.01E^{-7} - 20.9	Carbone <i>et al.</i> , 2007b; Pawar <i>et al.</i> , 2012
	p_x	0.79 ± 0.09		1.01E^{-7} - 20.9	
Prey-predator size scaling	k_0	0.109	kg	0.08 - 210.00	Peters, 1983
	p_k	1.16 ± 0.192		0.08 - 210.00	

1.2.2 Sensitivity analysis

To test the robustness of our predictions to variation in the scaling relationships and their parameterizations, we sampled each of the seven scaling exponents ($z, p_v, p_x, p_k, p_d, a_1, a_2$) from a Gaussian distribution with a standard deviation equal to the respective back-calculated standard error of the parameter estimate (Table S1).

2 Empirical Data

2.1 Activity budget data

We compiled data on daily activity budget (allocation of time among different activities in a day) in terrestrial carnivore species from published literature as well as existing databases. There are a variety of techniques for collecting activity budget data, including direct observation (Kruuk, 1972; Schaller, 1976), camera trapping (Bischof *et al.*, 2014), GPS collars (Eriksen *et al.*, 2011) and, more recently, accelerometers (Rozhnov *et al.*, 2011). These techniques differ in their time resolution of activity sampling, ability to detect activity when it occurs, and the definition of what comprises an activity — from radio signal strength (Do Linh San *et al.*, 2007) to number of photographs (Ridout & Linkie, 2009) to distance between successive GPS fixes (Miller *et al.*, 2014). To build a consistent, high-resolution database where measures durations could be directly compared between species, we restricted our data compilation to studies using radio tracking techniques (VHF, GPS collars or accelerometers). Camera trapping studies were excluded because it is difficult to estimate activity times accurately from snapshots, while studies using human observations were excluded because they were likely to underestimate the amount of time active.

For literature searches, we used a predefined set of keywords (“activity patterns”, “radio tracking”, “telemetry”, “gps collars”, “carnivore”), and preferentially selected studies reporting full 24 hours activity cycles based on one or more complete years of sampling. Because activity patterns are often reported as either graphs or figures, we used a digitizing software (Plot Digitizer v. 2.6, Huwaldt, 2014) to extract activity and time-stamp information. In order to express all quantities in SI units, activity patterns, time budgets and daily distance traveled data were converted to proportion of time spent active in the sampling interval (in seconds). We also recorded geographical location data from each study (longitude and latitude) to account for the effects of seasonality on the activity budget (see data analyses section below).

The best-represented Families in our dataset are Felids ($n = 14$ species), Canids ($n = 10$ species) and Mustelids ($n = 8$ species) (Fig. S2). Some terrestrial mammalian carnivore families were excluded from our data compilation either because of ecological or practical (i.e., lack of studies on activity, different methods used) reasons. In particular, vertebrate or invertebrate prey is not a major part of the diet of a number of species in the Order Carnivora. Ursids

(bears) are a good example — members of this family are the most omnivorous of all Carnivora (citealphunter2011carnivores, in Ripple *et al.*, 2014). Along with the giant panda’s (*Ailuropoda melanoleuca*) highly specialised diet (Schaller, 1985), the feeding ecology of many bear species features predominantly plant material, such as roots, fruits, nuts and seeds, as well as other non-meat resources. For instance, the diets of both the spectacled bear (*Tremarctos ornatus*) and grizzly bear (*Ursus arctos horribilis*) are dominated by various species of plants taken seasonally (Peyton, 1980; Munro *et al.*, 2006). For this reason, these species were left out of our analysis.

2.2 Intake Rate Data

Data on Intake rate were compiled from (Carbone *et al.*, 2007a, 1999) for 32 carnivores species. These data were reported as the daily energy intake (in $\text{kJ} \cdot \text{s}^{-1}$), which were then converted to $\text{J} \cdot \text{s}^{-1}$ for testing our model predictions for intake rate scaling.

2.3 Body mass measures and Size-ratio data

Average body weights of each species, when not available in the original publications, were taken from Table 7.1 in Gittleman (1989). Data on the average body weight of both carnivores species and their preferred prey were obtained from (Carbone *et al.*, 1999, 2007b) (41 species) and (Tucker & Rogers, 2014) (51 species).

2.4 Diet classification

Data on diet composition were compiled separately in the form of percentages of different food categories used by each species **Chris, need details on this from you, unless these details are published already elsewhere**. Based on the predominant type of food item ($>50\%$ of total diet composition), species were classified as either “carnivore”, “insectivore” or “omnivore”.

Average body size data for 63 predator species, and those of their preferred prey, were obtained from the published literature (Carbone *et al.*, 1999, 2007b; Tucker & Rogers, 2014). These were then categorically classified with respect to the their preferred prey: carnivore species preferentially feeding on large vertebrates were labelled as “large-prey eaters”. Conversely, the “small-prey eaters” category, included carnivores preferentially taking small vertebrates or invertebrates. Carnivores species showing a diet mixing two or more of these prey types were classified as “transitional species”.

2.5 Data Analyses

2.5.1 Accounting for pseudo-replicates

Many species data showed pseudo-replication because studies often sampled more than one individual at a time and multiple studies targeted the same species. When multiple measures of the activity budget were available, we took the geometric mean of the upper quantile (top 25%) of these pseudo-replicated values, both within and across studies. We were able to get a single average value of activity over 24 hours for each species in our dataset and then used it in all subsequent analyses (Supplementary Fig. S1c).

2.5.2 Activity budgets

We fitted three different models to the data to quantify the relationship between \log_{10} -transformed proportion of daily time active and body mass: ordinary least squares (OLS), a second degree (quadratic) polynomial model and a piecewise regression (package “segmented”, Muggeo 2008). The latter allows for testing of the existence of a breakpoint value in the data, as well as differences between the slopes of the regression lines on both sides of said breakpoint using the

201 Davies test (Muggeo, 2008). We selected the best fitting model using the small-sample Akaike
202 Information Criterion (AICc, Burnham & Anderson, 2002). All analyses were conducted in R
203 (v. 3.2.3, R Development Core Team, 2015) with significance level set as $\alpha = 0.05$.

Table S2: Three alternative models fitted to the activity time data as a function of Body Mass (m). AICc, Akaike Information Criterion corrected for small sample size.

Parameter	Linear	2 nd degree Polynomial	Piecewise
AICc	-23.258	-35.249	-37.167
r^2	0.036	0.349	0.425
a	-0.356 \pm 0.045	-0.397 \pm 0.023	-0.442, -0.156
b	-0.045 \pm 0.040	-0.189 \pm 0.138	
c			0.340 \pm 0.109
d			-0.197 \pm 0.051
t			0.534 \pm 0.138

a: intercept in the linear and polynomial models. *b*: slope of the 1st degree term in the linear and polynomial models. *c*: slope of the piecewise model below the breakpoint. *d*: slope of the piecewise model above the breakpoint. *t*: breakpoint found by the piecewise model

204 2.5.3 Accounting for seasonality in the Activity Data

205 Activity budget data are often collected over long periods of time, usually as long as radio-
206 tracking collars remain functional on the study subject or the study subject itself dies. As
207 such, the data we obtained from the literature often spanned months, if not years. As this
208 time scale, seasonality could conceivably play a role in determining how much time animals
209 spend active throughout the day, as resource availability can vary - sometimes dramatically -
210 from one season to the other. We accounted for this by analysing data from different seasons
211 separately, in order to test whether the pattern found by our main analyses held when the time
212 frame was reduced. As part of our literature review, we also collected data on which season
213 each study had taken place in and these were later categorised as either “resource rich”, if in
214 Spring or Summer, or “resource poor”, if in Winter or Autumn. Studies that reported data for
215 1+ years without providing details on seasons, were included in both datasets. Following the
216 same pattern from our main analyses, we fitted three model to each dataset: an OLS regression,
217 a polynomial model and a piecewise regression. The latter provided the better fit to the data
218 for both “rich” and “poor” seasons (Table S3), and also highlighted a similar pattern to that
219 observed in the main analyses (Fig. S3).

Table S3: Three alternative models fitted to the activity proportion data as a function of Body Mass (m), divided by season (see text above for details). Other specifications as in Table S2.

Parameter	Linear		2 nd degree Polynomial		Piecewise	
	Wet	Dry	Wet	Dry	Wet	Dry
AICc	-18.091	-19.638	-30.009	-7.747	-33.898	-29.241
r^2	0.028	0.023	0.366	0.254	0.478	0.370
a	-0.366 \pm 0.049	-0.383 \pm 0.048	-0.404 \pm 0.024	-0.477 \pm 0.034	-0.450, -0.138	-0.468, -0.191
b	-0.041 \pm 0.042	-0.036 \pm 0.042	-0.167 \pm 0.142	-0.254 \pm 0.197		
c					0.369 \pm 0.113	0.372 \pm 0.143
d					-0.210 \pm 0.052	-0.177 \pm 0.055
t					0.539 \pm 0.140	0.504 \pm 0.165

220 2.5.4 Intake Rate and Size Ratio data

221 Analyses of the Intake Rate and Size Ratio data were similar to those performed on the Activity
222 Proportion data. We used package “segmented” (Muggeo, 2008) in R v. 3.3.0 (R Development

Core Team, 2015) to fit a piecewise regression model to each dataset independently. When evidence of a breakpoint was found, we used the Davies' test (Muggeo, 2008) to test for significant differences in the slopes of the different segments of each the regression line separately.

Table S4: Three alternative models fitted to the intake rate data as a function of Body Mass (m). Other specifications as in Table S2.

Parameter	Linear	2 nd degree Polynomial	Piecewise
AICc	-0.748	-3.867	-7.290
r^2	0.906	0.922	0.935
a	1.113 ± 0.059	1.864 ± 0.036	1.093, 0.813
b	0.790 ± 0.046	3.777 ± 0.206	
c			0.514 ± 0.145
d			1.003 ± 0.076
t			0.573 ± 0.338

Table S5: Three alternative models fitted to the prey-predator size-ratio data as a function of Body Mass (m). Other specifications as in Table S2.

Parameter	Linear	2 nd degree Polynomial	Piecewise
AICc	197.5982	189.6485	187.001
r^2	0.4201	0.507	0.5447
a	-1.3449 ± 0.2063	-0.3458 ± 0.1313	-1.239, -2.737
b	1.2888 ± 0.1939	7.4548 ± 1.0425	
c			0.1975 ± 0.4355
d			2.4090 ± 0.3635
t			0.677 ± 0.199

Figure S1: **Steps in analysis of the empirical activity budget data.** **a:** Distribution of the raw activity proportion data against body size. **b:** Data averaged by species within individual studies, by taking the geometric mean of the upper quantile of the values reported. **c:** Finally, to obtain a single value of activity for each species included in our dataset we took the geometric mean of the upper quantile of the activity values reported by different studies.

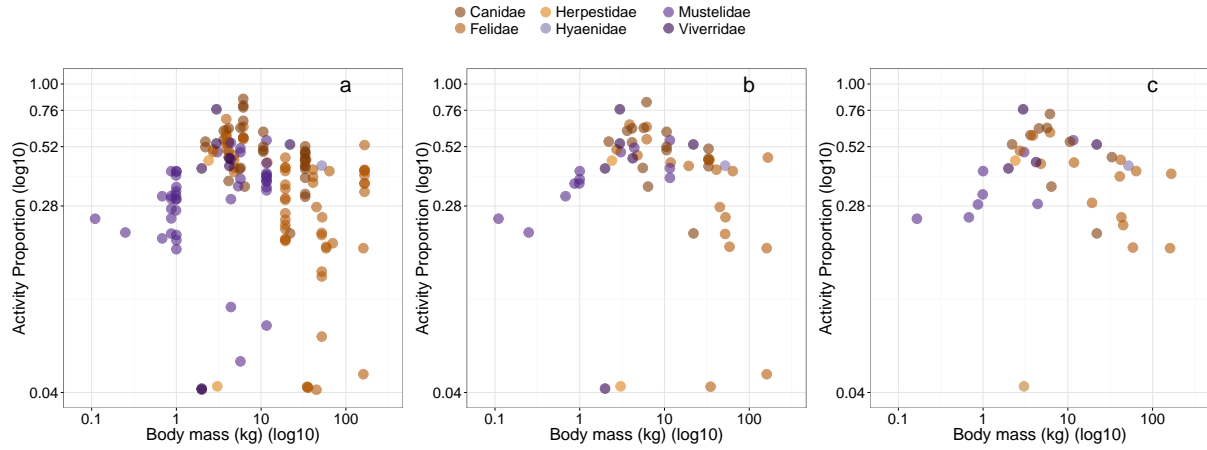


Figure S2: **Observed T_p for species belonging to three families.** Mustelids show a positive relationship between activity and body weight ($y = -0.496 + 0.177 \cdot x$, slope 95% CIs = (0.048, 0.305), $R^2 = 0.549$, $p = 0.0355$). Among Canids and Felids, the scaling of T_p is negative, with levels of activity decreasing as size gets larger (Canids, $y = -0.103 - 0.236 \cdot x$, slope 95% CIs = (-0.518, 0.046), $R^2 = 0.278$, $p = 0.144$; Felids, $y = -0.174 - 0.199 \cdot x$, slope 95% CIs = (-0.325, -0.074), $R^2 = 0.446$, $p = 0.00908$). Both axes are in log10-scale.

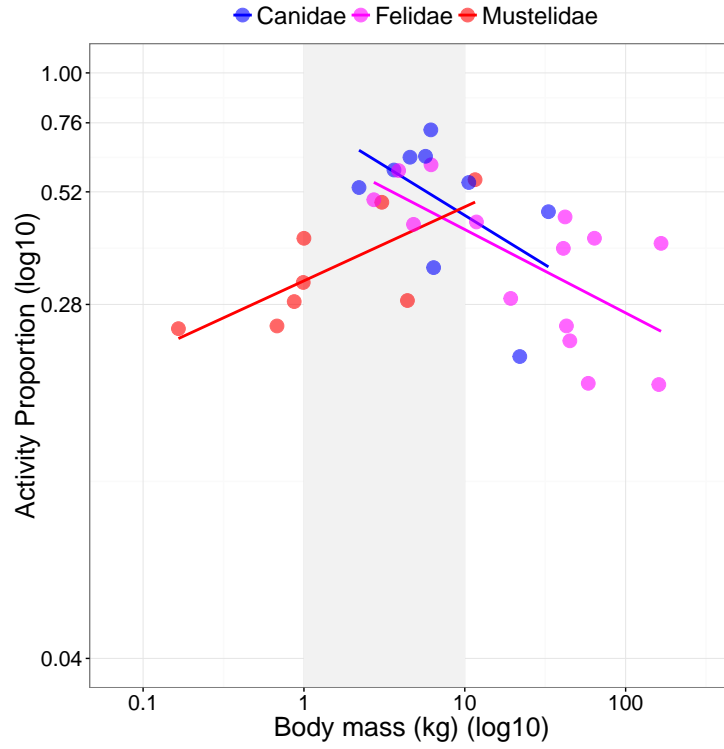
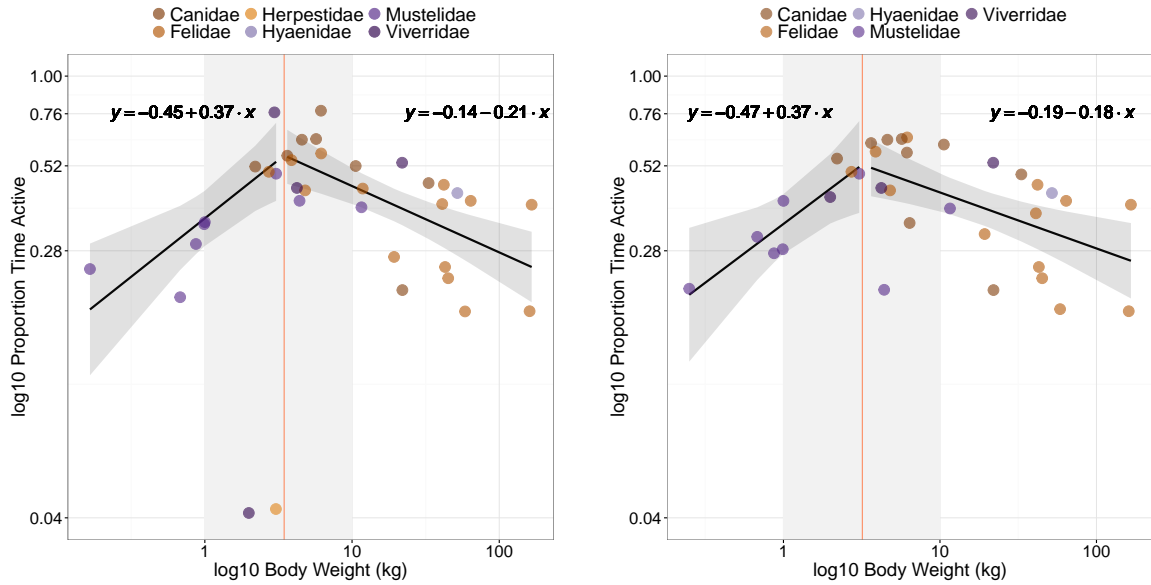


Figure S3: **Observed size scaling of T_p among Carnivores in “rich” and “poor” resource conditions.** **a:** “resource-rich” seasons. The breakpoint was found at 3.45 kg (95% CIs of 1.58, 5.34) and slopes of the two segments of the model on each side of this threshold value were significantly different (below breakpoint slope = 0.37 ± 0.11 , above breakpoint slope = -0.21 ± 0.05 , $p = 0.0002717$). Note that the two outliers with a T_p value of $\simeq 0.04$ were excluded from the analyses. **b:** “resource-poor” seasons. The breakpoint was found at 3.19 kg (95% CIs of 1.09, 5.30), with slopes that differed significantly from each other on each side of the flex point (below breakpoint slope = 0.37 ± 0.14 , above breakpoint slope = -0.18 ± 0.05 , $p = 0.003435$)



References

- Bischof, R., Ali, H., Kabir, M., Hameed, S. & Nawaz, M.a. (2014). Being the underdog: an elusive small carnivore uses space with prey and time without enemies. *J. Zool.*, 293, 40–48.
- Brown, J.H., Gillooly, J.F., Allen, A.P., Savage, V.M. & West, G.B. (2004). Toward a metabolic theory of ecology. *Ecology*, 85, 1771–1789.
- Burnham, K. & Anderson, D. (2002). *Model Selection and Multimodel Inference: A Practical Information-Theoretic Approach (2nd ed)*. vol. 172.
- Carbone, C., Mace, G., Roberts, S. & Macdonald, D. (1999). Energetic constraints on the diet of terrestrial carnivores. *Nature*, 402, 1997–2000.
- Carbone, C., Rowcliffe, J.M., Cowlishaw, G. & Isaac, N.J.B. (2007a). The scaling of abundance in consumers and their resources: implications for the energy equivalence rule. *Am. Nat.*, 170, 479–84.
- Carbone, C., Teacher, A. & Rowcliffe, J.M. (2007b). The costs of carnivory. *PLoS Biol.*, 5, e22.
- Dell, A.I., Pawar, S. & Savage, V.M. (2014). Temperature dependence of trophic interactions are driven by asymmetry of species responses and foraging strategy. *J. Anim. Ecol.*, 83, 70–84.
- Do Linh San, E., Ferrari, N. & Weber, J.M. (2007). Spatio-temporal ecology and density of badgers *Meles meles* in the Swiss Jura Mountains. *Eur. J. Wildl. Res.*, 53, 265–275.
- Eriksen, A., Wabakken, P., Zimmermann, B., Andreassen, H.P., Arnemo, J.M., Gundersen, H., Liberg, O., Linnell, J., Milner, J.M., Pedersen, H.C., Sand, H., Solberg, E.J. & Storaas, T. (2011). Activity patterns of predator and prey: a simultaneous study of GPS-collared wolves and moose. *Anim. Behav.*, 81, 423–431.
- Garland, T.J. (1983). Scaling the ecological cost of transport to body mass in terrestrial mammals. *Am. Nat.*, 121, 571–587.
- Gittleman, J.L. (1989). *Carnivore Behavior, Ecology, and Evolution*. 1st edn. Chapman & Hall Ltd, London.
- Gorman, M., Mills, M., Raath, J. & Speakman, J. (1998). High hunting costs make African wild dogs vulnerable to kleptoparasitism by hyaenas. *Nature*, 395, 1992–1994.
- Holling, C.S. (1966). The functional response of invertebrate predators to prey density. *Mem. Entomol. Soc. Canada*, 48, 1–86.
- Huwaldt, J.A. (2014). Plot Digitizer.
- Kolokotronis, T., Van Savage, Deeds, E.J. & Fontana, W. (2010). Curvature in metabolic scaling. *Nature*, 464, 753–6.
- Kruuk, H. (1972). *The Spotted Hyena: A Study of Predation and Social Behavior*. University of Chicago Press, Chicago, IL.
- Miller, C., Hebblewhite, M., Petrunenko, Y., Seryodkin, I., Goodrich, J. & Miquelle, D. (2014). Amur tiger (*Panthera tigris altaica*) energetic requirements: Implications for conserving wild tigers. *Biol. Conserv.*, 170, 120–129.
- Muggeo, V.M.R. (2008). segmented: An R package to Fit Regression Models with Broken-Line Relationships. *R News*, 8, 20–25.

267 Munro, R.H.M., Nielsen, S.E., Price, M.H., Stenhouse, G.B. & Boyce, M.S. (2006). Seasonal
268 and diel patterns of grizzly bear diet and activity in west-central Alberta. *J. {...}*, 87,
269 1112–1121.

270 Pawar, S., Dell, A.I. & Savage, V.M. (2012). Dimensionality of consumer search space drives
271 trophic interaction strengths. *Nature*, 486, 485–489.

272 Pawar, S., Dell, A.I. & Savage, V.M. (2015). From metabolic constraints on individuals to the
273 dynamics of ecosystems. In: *Aquat. Funct. Biodivers. An Ecol. Evol. Perspect.* (eds. Belgrano,
274 A., Woodward, G. & Jacob, U.). Elsevier, pp. 3–36.

275 Peters, R. (1983). *The ecological implications of body size*. 1st edn. Cambridge University Press,
276 Cambridge.

277 Peyton, B. (1980). Ecology , Distribution , and Food Habits of Spectacled Bears , *Tremarctos*
278 *ornatus* , in Peru. *J. Mammal.*, 61, 639–652.

279 R Development Core Team (2015). *R: A language and Environment for Statistical Computing*.
280 R Foundation for Statistical Computing, Vienna, Austria.

281 Ridout, M.S. & Linkie, M. (2009). Estimating overlap of daily activity patterns from camera
282 trap data. *J. Agric. Biol. Environ. Stat.*, 14, 322–337.

283 Ripple, W.J., Estes, J.a., Beschta, R.L., Wilmers, C.C., Ritchie, E.G., Hebblewhite, M., Berger,
284 J., Elmhagen, B., Letnic, M., Nelson, M.P., Schmitz, O.J., Smith, D.W., Wallach, A.D. &
285 Wirsing, A.J. (2014). Status and ecological effects of the world’s largest carnivores. *Science*,
286 343, 1241484.

287 Rozhnov, V.V., Hernandez-Blanco, J.a., Lukarevskiy, V.S., Naidenko, S.V., Sorokin, P.a., Litvi-
288 nov, M.N., Kotlyar, a.K. & Pavlov, D.S. (2011). Application of satellite collars to the study of
289 home range and activity of the Amur tiger (*Panthera tigris altaica*). *Biol. Bull.*, 38, 834–847.

290 Schaller, G.B. (1976). *The Serengeti lion: A study of predator-prey relations*. 1st edn. University
291 of Chicago Press, Chicago, IL.

292 Schaller, G.B. (1985). *Giant pandas of Wolong*. University of Chicago press.

293 Taylor, C.R., Heglund, N.C. & Maloiy, G.M. (1982). Energetics and mechanics of terrestrial
294 locomotion. I. Metabolic energy consumption as a function of speed and body size in birds
295 and mammals. *J. Exp. Biol.*, 97, 1–21.

296 Tucker, M.A. & Rogers, T.L. (2014). Examining predator-prey body size, trophic level and
297 body mass across marine and terrestrial mammals. *Proc. R. Soc. B*, 281, 20142103.